A Virtual Vehicle Based Coordination Framework For Autonomous Vehicles in Heterogeneous Scenarios

Ezequiel Debada, Laleh Makarem and Denis Gillet

***Abstract*—This work presents a novel *virtual vehicle* based decentralized coordination framework for Connected Autonomous Vehicles (CAVs). We explore the idea of CAVs being capable of positioning virtual vehicles to share their intended maneuver as well as request cooperation. This framework has potential to inspire versatile solutions and provides an intuitive interface to interact with reactive and unconnected vehicles. In this context, a preliminary coordination policy is proposed and tested on a three-legged single-lane roundabout. Simulation results show that the presented solution performs outstandingly better when it leverages the freedom at positioning virtual vehicles that our framework provides. Furthermore, the performance degradation resulting from mixing CAVs and unconnected cars is observed, and coordination assessment under this circumstance is discussed.**

I. Introduction

The fast growth of Autonomous Vehicles (AVs) technology shapes a future traffic scenario that seems far from being technologically homogeneous. Thus, decision-making policies for AVs have to account for the issues derived from the coexistence of vehicles with different levels of automation—referred here as *heterogeneous traffic* scenarios. In particular, this article tackles the problem of coordination of AVs at intersections, which has attracted a great deal of attention over the last decades.

A broad range of centralized solutions can be found in the literature. Since Peter Stone proposed his *autonomous intersection management* protocol [1], reservation algorithms have been extensively used in the literature [2]. Over the last years, optimization-based policies have arisen, which range from techniques covering *planning* and *control* at once [3], to priority-based approaches where the relative priorities between vehicles are assumed to be given [4].

Decentralized control schemes have been applied likewise. Reactive coordination protocols are popular in the literature because of its low computational burden. Solutions based on *navigation functions* [5], *virtual vehicles* [6] or *virtual platoons* [7] have been presented in the past. Optimization has also been exploited in decentralized form. Solutions that assume that relative priorities between vehicles are given [8] or that the optimization order is known [9] have been proposed. Recently, game theory concepts have been applied to address coordination of vehicles [10].

Although coordination on heterogeneous traffic conditions has started raising awareness, there are only a few works on the topic [11]. Typically, coordination strategies are designed for homogeneous cases and then adapted to heterogeneous ones—which presumes that performing well in the former cases is required to do so in the latter ones. We claim that coordination solutions for heterogeneous scenarios should not be directly inherited from homogeneous cases as they do not present the same dynamics.

In this article, a *virtual vehicle* based coordination framework for Connected Autonomous Vehicles (CAVs) is proposed, whereby a simple interface with unconnected and reactive cars is provided. The concept of *virtual vehicle* denotes techniques that exploit *phantom vehicles* to reach cooperation among CAVs, and it was first presented in [6], where virtual vehicles were generated by mapping cars on their targeted lane. This criterion is also used in [12] and is slightly extended in [7] by making use of *scaled traveled distances* to generate virtual vehicles.

The main contribution of this paper is the formulation of a novel coordination framework for CAVs in heterogeneous conditions, which is tested on a single-lane roundabout scenario. The concept of *virtual vehicles* is extended by allowing CAVs to control the state of their virtual vehicle, which is then broadcast. Moreover, solutions are provided to deal with the limitations stemming from the coexistence of CAVs and unconnected and reactive cars. Lastly, based on our simulation results, coordination assessment in heterogeneous scenarios is briefly discussed.

This manuscript is organized as follows. Firstly, the proposed framework is presented in Section II. Specifics concerning the coordination policy are then given in Section III. Section IV describes the case study used to generate the results shown in Section V. Finally, Section VI gathers some conclusions and future research directions.

II. Coordination framework

We propose a framework based on the idea of using virtual vehicles to represent the maneuvers that vehicles aim to perform. These virtual vehicles are referred to as *projected vehicles* (or *projections* in short), making reference to the fact that they represent a maneuver intended to be performed in the future. In this context, a vehicle would navigate considering the projected vehicles of surrounding cars and would perform maneuvers by generating its projection. Vehicle to vehicle communication is exploited by considering that some CAVs can explicitly broadcast the state of their projection. Hence they can freely position it at any spot of interest.

This framework aims at scenarios where three types of vehicles coexist: *unconnected vehicles*, *reactive* CAVs (rCAVs), and *anticipative* CAVs (aCAVs). *Unconnected vehicles* category gathers human-driven cars and unconnected AVs. The term *rCAVs* denotes CAVs that share their current state and can interpret any incoming information. Moreover,

Ezequiel Debada, Laleh Makarem and Denis Gillet are with the Coordination and Interaction Systems (React) group at École Polytechnique Fédérale de Lausanne (EPFL). Emails: {ezequiel.gonzalezdebada, laleh.makarem, denis.gillet } @epfl.ch

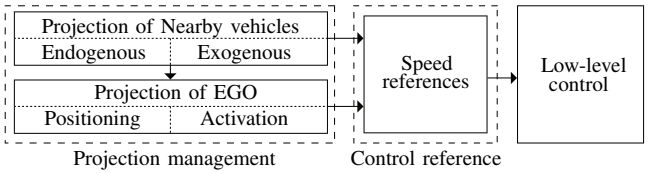

Fig. 1. Coordination framework scheme.

term *aCAVs* refers to CAVs able to broadcast not only their current state but also that of its projection.

The fact that different kinds of vehicles are considered allows classifying projections w.r.t. the source of information they stem from. In this line, a projection is referred to as *exogenous* when its position is explicitly broadcast by its owner, i.e. it belongs to another CAVs. On the contrary, when a projection represents the maneuver of an unconnected vehicle, it has to be inferred from the context, and it is called *endogenous projection*.

In subsequent sections, the framework is presented from the egocentric standpoint of an aCAV, and the term *EGO vehicle* (or *EGO* in short) is used to denote the vehicle performing the described computations. A schematic representation of the framework is shown in Figure 1, where two main blocks are differentiated: *projection management* and *control reference*. First, projections of nearby cars are generated/received to model their intended maneuvers. These projections are taken into account by EGO to calculate the location of its projected vehicle, which is broadcast when it is activated—meaning that a suitable spot to place the projection was found. Afterward, *speed references* for EGO and its projection are calculated and tracked by low-level controllers. We assume in the rest of this manuscript that these references can be perfectly followed.

The objective of this architecture is twofold. On the one hand, the freedom of aCAVs to position their projection potentially allows reaching cooperation in more intricate situations—as the cooperation effort can be whereby decreased. On the other hand, it provides a simple way for CAVs to interact with unconnected vehicles. Specifics and further details are provided in §III.

A. Notation

Let us consider a generic traffic scenario with N cars (set $\mathcal{V} : |\mathcal{V}| = N$). Vehicles can be rCAVs, aCAVs, or *unconnected* vehicles and are represented by the sets $\mathcal{A}^{\mathrm{r}} : |\mathcal{A}^{\mathrm{r}}| = N_{\mathrm{r}}$, $\mathcal{A}^{\mathrm{a}} : |\mathcal{A}^{\mathrm{a}}| = N_{\mathrm{a}}$, and $\mathcal{U} : |\mathcal{U}| = N_{\mathrm{u}}$ respectively. Similarly, sets $\mathcal{V}_i \subseteq \mathcal{V}$, $\mathcal{U}_i \subseteq \mathcal{U}$, $\mathcal{A}^{\mathrm{r}}_i \subseteq \mathcal{A}^{\mathrm{r}}$ and $\mathcal{A}^{\mathrm{a}}_i \subseteq \mathcal{A}^{\mathrm{a}}$ show the subsets of all vehicles, unconnected cars, rCAVs and aCAVs respectively, that vehicle i can perceive.

A vehicle $i \in \mathcal{A}^{\mathrm{a}}$ has to generate its projection i_{p}, assign an endogenous projection j_{n} to every car $j \in \mathcal{U}_i \cup \mathcal{A}^{\mathrm{r}}_i$, and an exogenous one j_{x} to vehicles $j \in \mathcal{A}^{\mathrm{a}}_i$. Notice that, in this paper, the term *vehicle* makes reference to both projected and real vehicles if not stated otherwise. Moreover, the terms $\prec i$ and $\succ i$ denote the first vehicle behind and ahead vehicle i.

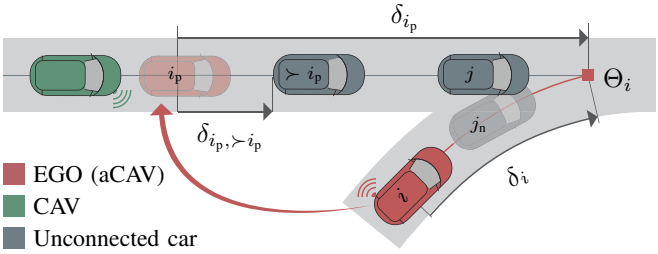

Fig. 2. EGO (vehicle i) performing a merging maneuver by placing projection i_{p} right ahead another CAV, which can cooperate by reacting to it. The point before which the maneuver has to end is denoted Θ_i.

III. Preliminary Coordination Policy

This section presents a preliminary approach to address *projection management* and *speed reference* generation problems from the standpoint of aCAVs.

Without lack of generality, spatially constrained maneuvers (Figure 2) are considered, yet the discussion can be adapted to other situations through the appropriated modifications.

A. Projection management

The *projection management* problem for a vehicle $i \in \mathcal{A}^{\mathrm{a}}$ (EGO vehicle) consists in positioning and activating a projection i_{p} to perform maneuvers as well as endogenous and exogenous projections of vehicles $j \in \mathcal{A}^{\mathrm{r}}_i \cup \mathcal{U}_i$ and $j \in \mathcal{A}^{\mathrm{a}}_i$ to represent the intended maneuver of nearby vehicles. The position of a vehicle i is given by its distance δ_i to the point Θ_i where the maneuver has to end (Figure 2). By an abuse of notation, the distance between vehicles i and j is similarly termed $\delta_{i,j}$. Besides, the fact that a maneuver is being performed (termed *activation state*) is denoted by the binary variable γ_i, showing whether vehicle i is performing its targeted maneuver ($\gamma_i = 1$) or not ($\gamma_i = 0$).

1) Endogenous projections: Endogenous projections j_{n} are required to cooperate with vehicles $j \in \mathcal{U}_i \cup \mathcal{A}^{\mathrm{r}}_i$ and are simply positioned on the targeted lane of vehicle j with

$$\delta_{j_{\mathrm{n}}} = \delta_j \,. \tag{1}$$

Additionally, j_{n} is considered to be active only when vehicle j has started the maneuver, which is shown by the variable $\gamma_{j_{\mathrm{n}}}$ inferred from the state of the lane change indicator if vehicle $j \in \mathcal{U}_i$, or explicitly broadcast ($\gamma_{j_{\mathrm{x}}}$) if $j \in \mathcal{A}^{\mathrm{r}}_i$.

2) Exogenous projections: Exogenous projections are assigned to vehicles $j \in \mathcal{A}^{\mathrm{a}}_i$ and are fully defined by $\delta_{j_{\mathrm{x}}}$ and $\gamma_{j_{\mathrm{x}}}$, which are broadcast by vehicle j.

3) Projection of EGO: EGO (vehicle $i \in \mathcal{A}^{\mathrm{a}}$) makes use of a projection to communicate its intention and request cooperation to surrounding CAVs. Thus, positioning policies have to account for (i) the communication capabilities of surrounding vehicles and (ii) some decision-making criterion.

On the one hand, the projected vehicle of EGO has to be placed right ahead a vehicle able to perceive it. On the other hand, a decision-making criterion has to be defined to perform the targeted maneuver. In this work, an estimation of the requested *cooperation effort* is used to determine whether it is feasible to place a projection at a certain spot or not.

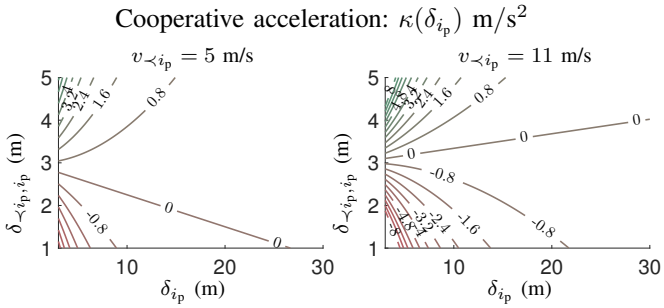

Fig. 3. Value of κ (6) considering a follower $\prec i_p$ driving at $v_{\prec i_p}$ m/s. Common parameters for both plots are $v_{\succ i} = 8$ m/s and $\sigma_i = 3$ s.

The cooperation effort is measured through the maximum acceleration that vehicle $\prec i_p$ can apply over time such that the headway $s_{\prec i_p, i_p}$ is above the *critical gap* σ_i by the time it reaches Θ_i. This acceleration is named *cooperative acceleration* and denoted as $\kappa(\delta_{i_p})$, where its dependence with δ_{i_p} is explicitly expressed. Notice that in general, $s_{j,i}$ represents the time between the position δ_i and vehicle j, and is calculated as

$$s_{j,i} = \frac{\delta_{j,i}}{v_j} \,. \tag{2}$$

To calculate κ as a function of δ_{i_p}, the time τ_i at which the gap reaches Θ_i is first estimated as

$$\tau_i = \frac{\delta_{i_p}}{v_{\succ i_p}} \,, \tag{3}$$

where $v_{\succ i_p}$ shows the average speed vehicle $\succ i_p$ is expected to follow. Then, assuming that $\prec i_p$ will apply in average the acceleration $a_{\prec i_p}$, the estimated headway $\hat{s}_{\prec i_p, i_p}$ at τ_i is

$$\hat{s}_{\prec i_p, i_p} = \frac{\delta_{\prec i_p, i_p} + \delta_{i_p} - \left(v_{\prec i_p}\tau_i + a_{\prec i_p}\tau_i^2/2\right)}{v_{\prec i_p} + a_{\prec i_p}\tau_i} \,. \tag{4}$$

To impose $\hat{s}_{\prec i_p, i_p} \geq \sigma_i$, constraint

$$a_{\prec i_p} \leq \frac{\delta_{\prec i_p, i_p} + \delta_{i_p} - v_{\prec i_p}\left(\tau_i + \sigma_i\right)}{\tau_i^2/2 + \sigma_i\tau_i} \tag{5}$$

has to be fulfilled. The right side of the equation represents the *cooperative acceleration* $\kappa(\delta_{i_p})$. From (3) and (5), and exploiting the fact that $\delta_{\prec i_p, i_p} = \delta_{\prec i_p} - \delta_{i_p}$, the next can be written

$$\kappa(\delta_{i_p}) = \frac{2v_{\succ i_p}^2\left(\delta_{\prec i_p} - v_{\prec i_p}\left(\delta_{i_p}/v_{\succ i_p} + \sigma\right)\right)}{\delta_{i_p}^2 + 2\sigma v_{\succ i_p}\delta_{i_p}} \,. \tag{6}$$

In Figure 3, κ is shown for two different sets of parameters. These graphs highlight the fact that as δ_{i_p} increases, nearby vehicles would have to brake less to cooperate.

The projected vehicle of EGO is positioned as follows. On the one hand, while the maneuver is being performed ($\gamma_{i_p} = 1$), its position at $t_1 \geq t_0$ is given by

$$\delta_{i_p}(t_1) = \delta_{i_p}(t_0) + \int_{t_0}^{t_1} \overline{v}_{i_p}(t|t_0)\ \mathrm{d}t \,, \tag{7}$$

where $\overline{v}_{i_p}(t|t_0)$ is the speed profile (calculated at t_0) that projection i_p has to follow. On the other hand, when projected vehicle is not active—meaning that a suitable location has not been found yet—the position is the result of the next optimization problem

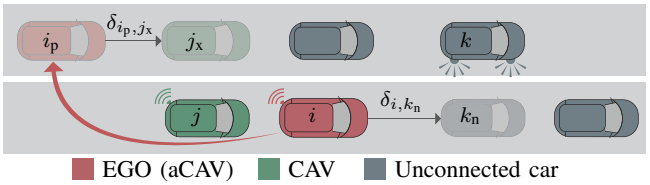

Fig. 4. Relevant vehicles to be taken into account by vehicle $i \in \mathcal{A}^a$ when calculating speed references $\overline{v}_i$ and $\overline{v}_{i_p}$ to perform a lane change maneuver.

$$\min \delta_{i_p} \tag{8}$$
$$\text{s.t. } \delta_{i_p} \geq \underline{\delta}_{i_p} \tag{9}$$
$$\prec i_p \in \mathcal{A}^r \cup \mathcal{A}^a \text{ if } \delta_{i_p} > \delta_{i_n} \tag{10}$$
$$\kappa(\delta_{i_p}) \geq \kappa_i^* \,. \tag{11}$$

This problem aims to find the closest suitable position considering constraints (9)-(11). Constrain (9) limits to

$$\underline{\delta}_{i_p} = v_{\succ i_p}\underline{\tau}_i \tag{12}$$

the closer the projection i_p can be to Θ_i. In (12), $v_{\succ i_p}$ is used as the expected average circulating speed in the targeted lane, and $\underline{\tau}_i$ designates the minimum time the real vehicle needs to reach Θ_i. The latter can be simply estimated by using the kinematics equation for uniformly accelerated motion as

$$\underline{\tau}_i = \frac{v_i + \sqrt{v_i^2 + 2\overline{\alpha}_i\delta_i}}{\overline{\alpha}_i} \,, \tag{13}$$

where $\overline{\alpha}_i$ denotes the maximum positive acceleration.

Then, constraint (10) makes sure that the first following vehicle $\prec i_p$ can interpret projected vehicles if required. Notice that placing a projection i_p with $\delta_{i_p} \leq \delta_{i_n}$ does not represent any problem w.r.t. vehicles $j \in \mathcal{U}_i$. In fact, in that case, these are expected to overreact by considering the endogenous projection i_n.

Lastly, constraint (10) imposes the cooperative acceleration to be above a threshold κ_i^*. Meaning that the *cooperation effort* that a vehicle requests to nearby vehicles is upper bounded.

The activation of the projected vehicle is done through

$$\gamma_i = \begin{cases} 1 & \text{if } \delta_{i,\succ i} \geq \delta_i \wedge \exists \delta_{i_p} \\ 0 & \text{otherwise} \end{cases} \,. \tag{14}$$

That is, the maneuver starts only if a suitable position was found and there is no vehicle between vehicle i and Θ_i.

Notice that, even though two CAVs could generate projections at the same spot, it does not represent any problem. In practice, as two real vehicles cannot occupy the same physical location, one of the two conflicting projections reaches the point that defines the end of its maneuver before than the other. Consequently, one vehicle would perform the maneuver while the other would control the projection to fit in the closest existing gap.

B. Speed reference

Once the projected vehicle is placed and active, the speed references $\overline{v}_i$ and $\overline{v}_{i_\mathrm{p}}$ followed by vehicles i and i_p have to be calculated. Vehicles $j \in \mathcal{V}_i$ and their projections (j_p, j_x or j_n according to the case) have to be considered to that end (Figure 4). Speed references should allow vehicles i and i_p to follow the traffic stream on their lanes, and merge when the maneuver ends.

The preliminary solution presented here solves in-lane navigation by implementing a state-of-the-art car-following model, for which the distance up to the first perceptible vehicle will be used. Moreover, a coupling strategy is addressed to link $\overline{v}_i$ and $\overline{v}_{i_\mathrm{p}}$ while a maneuver is being performed. In this line, we propose the use of a car-following model to obtain $\overline{v}_{i_\mathrm{p}}$ first and then computing $\overline{v}_i$ according to it. This section presents the car-following model used in simulation as well as a preliminary coupling strategy.

1) Car-following model: A simplified version of Gipps car-following model [13] is used here. Notice that, in this work, surrounding projections and real cars are equally considered notwithstanding that they represent soft and hard constraints respectively.

The used car-following model applies the maximum acceleration to either reach a desired speed or keep a safe distance with the first vehicle ahead. According to it, the speed reference $\overline{v}_i(t|t_0)$ of vehicle i is calculated as

$$\overline{v}_i(t|t_0) = \min\left(v_i(t_0) + \overline{\alpha}(t-t_0), \nu_i, v_i^{\mathrm{s}}(t|t_0)\right) , \tag{15}$$

where

$$v_i^{\mathrm{s}}(t|t_0) = \underline{\alpha} T_i + \sqrt{v_{\succ i}^2(t|t_0) + \underline{\alpha}^2 T_i^2 - 2\underline{\alpha}(\delta_{i,\succ i}(t|t_0) - \eta_i)} \tag{16}$$

is the speed that allows keeping a safe distance with the next vehicle on the lane. In Equations (15)–(16), T_i represents *reaction time*, maximum positive and negative accelerations are denoted by $\overline{\alpha}$ and $\underline{\alpha}$, and η_i shows the minimum inter-vehicle distance. Moreover $v_{\succ i}(t|t_0) = v_{\succ i}(t_0)$, and

$$\delta_{i,\succ i}(t|t_0) = \delta_{i,\succ i}(t_0) + (v_{\succ i}(t_0) - v_i(t_0))(t-t_0) . \tag{17}$$

Notice that, by using $\delta_{i,\succ i}$ in (16) we consider that CAVs react to active projections as if they were real vehicles.

2) Coupling: A coupling strategy is needed to control a real vehicle i and its projection i_p while performing a maneuver. The target being making the projected and real vehicles reach Θ_i at the same time with the same speed.

To do that, we consider $\overline{v}_{i_\mathrm{p}}(t|t_0)$ to be given by the car-following model described in (15)–(16). The speed reference profile $\overline{v}_i(t|t_0)$ is then calculated as

$$\overline{v}_i(t|t_0) = \min\left(\nu_i, \overline{v}_{i_\mathrm{p}}(t|t_0)\omega(t|t_0)\right) . \tag{18}$$

In this Equation, $\omega(t|t_0)$ with $t \in [t_0, \mu_i]$ is the coupling coefficient calculated at t_0, which takes the form

$$\omega(t|t_0) = \max\left(0, \beta_1(t-\mu_i)^2 + \beta_2(t-\mu_i) + 1\right) , \tag{19}$$

where $\mu_i = t_0 + \tau_i$ and β_1 and β_2 are tuning coefficients that are updated at every sampling time. This formulation makes $\omega(\mu_i|t_0) = 1$, which imposes $v_i(\mu_i|t_0) = v_{i_\mathrm{p}}(\mu_i|t_0)$ in (18). That is, both vehicles finalize the maneuver at time μ_i with the same speed.

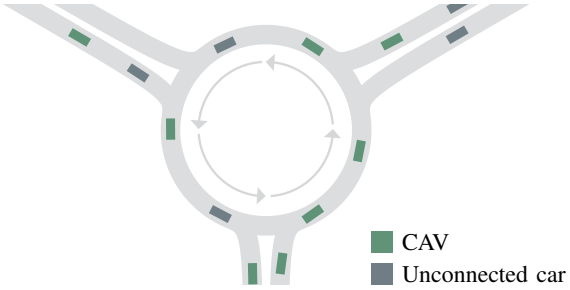

Fig. 5. Three-legged single-lane roundabout.

Coefficients β_1 and β_2 are computed by considering

$$\left.\frac{\mathrm{d}\ \omega(t|t_0)}{\mathrm{d}\ t}\right|_{t_0} = 0 , \tag{20}$$

and the fact that vehicle i has to travel δ_i meters in τ_i seconds

$$\int_{t_0}^{\mu_i} v_{i_\mathrm{p}}(t|t_0)\omega(t|t_0)\ \mathrm{d}t = \delta_i . \tag{21}$$

A preliminary result is obtained by assuming that $v_{i_\mathrm{p}}(t|t_0)$ in (21) is in average equal to $v_{\succ i_\mathrm{p}}(t_0)$, what leads to

$$\begin{bmatrix} \beta_1 \\ \beta_2 \end{bmatrix} = \begin{bmatrix} \frac{\tau^3 v_{\succ i_\mathrm{p}}}{3} & \frac{\tau^2 v_{\succ i_\mathrm{p}}}{2} \\ -2\tau_i & 1 \end{bmatrix}^{-1} \begin{bmatrix} \delta_i - v_{\succ i_\mathrm{p}}\tau_i \\ 0 \end{bmatrix} . \tag{22}$$

One direct consequence of applying this strategy is that the maximum speed in (15), when it refers to i_p, takes the value

$$\nu_{i_\mathrm{p}}(t_0) = \nu_i(t_0)\omega(t_0|t_0) . \tag{23}$$

IV. Case Study

In this manuscript, a *three-legged single-lane roundabout* is used to test the proposed coordination policy (Figure 5). Roundabouts are particularly convenient in this context as their natural working principle requires gaps generation, and the entering maneuver is spatially constrained. They are also challenging scenarios cooperative wise, due to their geometry and complex interaction between conflicting traffic streams [14].

Following sections describe the behavioral models used to simulate rCAVs and unconnected cars in our scenario and provide further details concerning information flow.

A. Reactive CAVs

Conceptually, rCAVs can interpret any incoming information (hence able to generate exogenous projections) but are not able to freely generate projected vehicles. In practice, a vehicle $i \in \mathcal{A}^{\mathrm{r}}$ is modeled as an aCAV whose projection is placed according to

$$\delta_{i_\mathrm{p}} = \delta_i . \tag{24}$$

The activation in this case follows

$$\gamma_i = \begin{cases} 1 & \text{if } \delta_{i,\succ i} \geq \delta_i \wedge \kappa(\delta_{i_\mathrm{p}}) \geq \kappa_i^* \\ 0 & \text{otherwise} \end{cases} . \tag{25}$$

Regarding *speed reference* generation, the approach described in §III-B is applied.

TABLE I. PERCEPTIBLE VEHICLES

EGO	Nearby vehicle		
	$j \in \mathcal{U}$	$j \in \mathcal{A}^{\mathrm{r}}$	$j \in \mathcal{A}^{\mathrm{a}}$
Unconnected veh.	$j,\ j_{\mathrm{n}}$	$j,\ j_{\mathrm{n}}$	$j,\ j_{\mathrm{n}}$
RCAVs	$j,\ j_{\mathrm{n}}$	$j,\ j_{\mathrm{n}}$	$j,\ j_{\mathrm{x}}$
aCAVs	$j,\ j_{\mathrm{n}}$	$j,\ j_{\mathrm{n}}$	$j,\ j_{\mathrm{x}}$

B. Unconnected vehicles

Unconnected vehicles are supposed to exhibit human-alike-driver behavior, which is here modeled as a combination of car-following and gap-acceptance models.

For the sake of consistency, gap-acceptance criterion is formulated in terms of *projection management*. Thus, a vehicle $i \in \mathcal{U}$ behaves as if its projection was placed according to (24) and activated following

$$\gamma_i = \begin{cases} 1 & \text{if } \delta_{i,\succ i} \geq \delta_i \wedge s_{\prec i_{\mathrm{p}},i_{\mathrm{p}}} \geq \sigma_i \wedge s_{i,\succ i} \geq \phi_i \\ 0 & \text{otherwise} \end{cases}, \quad (26)$$

where σ_i and ϕ_i stand for the *critical gap* and *follow-up* times for vehicle i respectively. Moreover, $s_{\prec i_{\mathrm{p}},i_{\mathrm{p}}}$ and $s_{i,\succ i}$ (2) designate the headway and follow-up time.

The implemented car-following model is the one exposed in §III-B (Equations (15)-(16)) except the reaction time is increased, and the intention of surrounding aCAVs are modeled through endogenous projections.

C. Information flow

The set of projected and real vehicles perceived by every type of vehicle is represented in Table I. Notice that when unconnected vehicles (set $\mathcal{U}$) are involved in the information exchange, the two involved vehicles have to be within the field of view of each other. Moreover, since vehicles in $\mathcal{U}$ are unconnected, they cannot assign exogenous projections to aCAVs. Furthermore, they are assumed to interpret correctly the lane change indicators of nearby vehicles.

V. RESULTS

In this section, simulation results based on the case study presented in §IV are shown and discussed. We first gather the values of all used parameters. Critical gap and follow up times are $\sigma = 2$ s and $\phi = 1$ s. Acceleration bounds are considered $\overline{\alpha} = 3\ \mathrm{m/s^2}$ and $\underline{\alpha} = -3\ \mathrm{m/s^2}$ and the *cooperative acceleration* threshold is $\kappa^* = 1\ \mathrm{m/s^2}$. Maximum speed is assumed to be $\nu_i = 15\ \mathrm{m/s}$. Ultimately, the minimum distance considered safe is $\eta_i = 3$ and reaction time T_i takes value 0.5 s if $i \in \mathcal{A}^{\mathrm{r}} \cup \mathcal{A}^{\mathrm{a}}$ and 1 s if $i \in \mathcal{U}$.

We carried out simulations of 40 scenarios (with different traffic load) where the instant at which vehicles arrive were generated by using a Poisson distribution. Incoming traffic is evenly distributed among the legs of the roundabout. Besides, origin-destination patterns are uniformly drawn considering the probability of taking the first, second and third exits being 20%, 60%, and 20% respectively. For each scenario, 6 cases with different vehicles combinations were simulated. Details are shown in Table II, where two groups (homogeneous and heterogeneous cases with a CAVs penetration ratio of 50%) are differentiated. Figure 6 shows the throughput values registered in each simulated case.

TABLE II. CASES: NUMBER AND TYPE OF CONSIDERED VEHICLES

Case	1	2	3	4	5	6
N_{u}	200	-	-	100	100	100
N_{r}	-	200		100	-	50
N_{a}	-		200	-	100	50

In cases 1–3 (upper plot in Figure 6), where homogeneous scenarios were tested, aCAVs report the best throughput in 39 scenarios out of 40. Heterogeneous cases 4–6 (lower plot in Figure 6) show that mixing CAVs with human-alike-driven vehicles always improves coordination w.r.t. case 1 (where only unconnected vehicles are considered).

A fundamental performance result shown in Figure 6 is the radically different trend observed in homogeneous and heterogeneous conditions. On the one hand, the throughput values in cases 2–3 are significantly reduced when unconnected vehicles are introduced (cases 4–5). Interestingly, while our algorithm reports the best throughputs in homogeneous conditions, no difference between tested approaches is observed in the simulated heterogeneous scenarios.

In an attempt to understand the positive effect of aCAVs in homogeneous cases and how it degrades with traffic heterogeneity, an indicator composed of pairs: *waiting time-circulating speed* is explored. This indicator is expected to provide information concerning entering-circulating flow balance. For each case, a set of samples $\mathcal{S} = \{i\}$ (associated to pairs (w_i, v_i^{c}) *waiting time-circulating speed*) were collected. The probability $\mathrm{P}(w, v^{\mathrm{c}})$ was then represented through 2D histograms, whose contour plots are shown in Figure 7. Every area $i \in [1, 4]$ therein included (differentiable by its color) illustrates the subset

$$\mathcal{S}_i = \{j \in \mathcal{S} | p_i \leq \mathrm{P}(w_j, v_j^{\mathrm{c}}) \leq p_{i+1}\}, \quad (27)$$

where p_i is the ith element of vector $\mathbf{p} = [0.1, 0.3, 0.5, 0.7, 0.99]$.

Clearly differentiable patterns are observed for aCAVs and rCAVs in homogeneous conditions (upper plots in Figure 7). These patterns show that the performance of our algorithm in heavy traffic and homogeneous conditions is due to a balanced waiting time distribution and a moderate circulating speed. These two effects can be attributed to the *scanning* and *booking* processes performed when an aCAV places its projection. On the one hand, being able to scan the full roundabout helps to find a suitable position sooner. On the other hand, as the number of projected and real vehicles within the intersection increases and becomes more stable, the resulting circulating speed is more steady and moderate.

In heterogeneous scenarios, the patterns (lower plots in Figure 7) are substantially different compared to homogeneous cases. It is clear that human-alike-driven vehicles add dynamics that are not present in homogeneous scenarios. Given the remarkable drop of performance, this issue is worth being studied separately.

Two aspects were not evaluated here: the origin-destination pattern as well as the number and distribution of CAVs in the scenario. The origin-destination pattern could be claimed not to cause the radical drop in performance since it did not prevent the clear differences in homogeneous cases from appearing. Therefore, CAVs penetration and distribution could be responsible for such degradation. This aspect,

Fig. 6. Throughput for cases 1–3 and cases 4–6 (upper and lower plot respectively), where cases differ in the included type of vehicles (Table II).

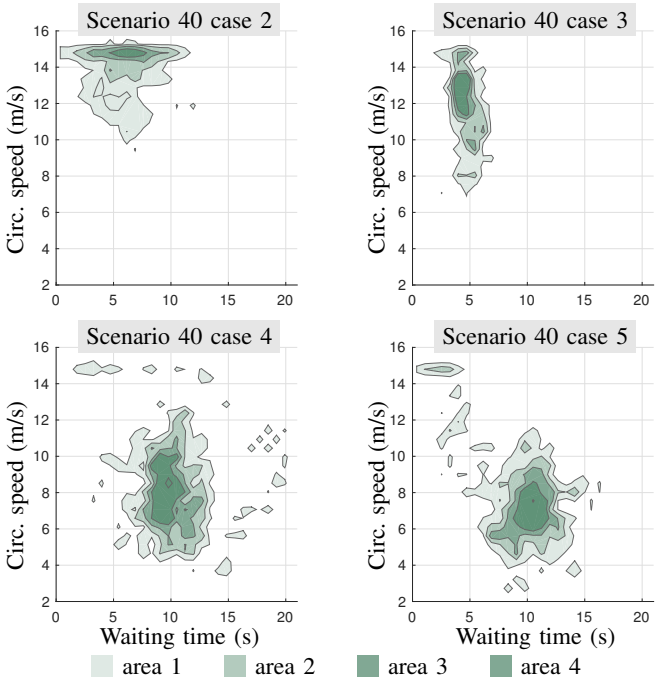

Fig. 7. Contour plots of *waiting time-circulating speed* 2D histograms for four selected cases (Table II). Every area i represents the subset $\mathcal{S}_i$ (27) containing the samples whose probability of appearance is between p_i and p_{i+1}. With p_i being the i-element of vector $\mathbf{p} = [0.1, 0.3, 0.5, 0.7, 0.99]$.

as well as its importance in designing reliable coordination policies in heterogeneous conditions, are subjects of ongoing investigations.

VI. Conclusions and Future Work

In this work, a coordination framework for connected autonomous vehicles, based on the concept of *virtual vehicles*, is proposed. The framework provides a suitable interface to reach coordination between vehicles with uneven technological capabilities. Additionally, a preliminary coordination policy has been formulated and assessed in simulation.

Cases where CAVs have freedom to place their projected vehicles outperform cases where projected vehicles must be inferred from the context. The assessment of waiting time and circulating speed shows that our algorithm moderates circulating speed and balances waiting time in heavy traffic conditions, which results to be a suitable operation regime for the treated intersection. This feature is remarkably degraded when human-alike driven cars are introduced, which stresses that heterogeneous scenarios present new dynamics w.r.t. homogeneous cases. Thus, appropriate techniques to assess and design coordination algorithms have to be investigated.

The study of coordination policies that account for origin-destination patterns as well as the expected behavior of the traffic stream is subject of ongoing research.

VII. Acknowledgments

The investigations leading to these results was co-funded by the international chair DriveForAll.

References

[1] D. Fajardo, T.-C. Au, S. Waller, P. Stone, and D. Yang, "Automated intersection control: Performance of future innovation versus current traffic signal control," *Transportation Research Record: Journal of the Transportation Research Board*, no. 2259, pp. 223–232, 2011.

[2] K. Zhang, D. Zhang, A. de La Fortelle, X. Wu, and J. Grégoire, "State-driven priority scheduling mechanisms for driverless vehicles approaching intersections," *IEEE Transactions on Intelligent Transportation Systems*, vol. 16, no. 5, pp. 2487–2500, 2015.

[3] L. Riegger, M. Carlander, N. Lidander, N. Murgovski, and J. Sjöberg, "Centralized mpc for autonomous intersection crossing," in *Intelligent Transportation Systems (ITSC), 2016 IEEE 19th International Conference on*. IEEE, 2016, pp. 1372–1377.

[4] J. Gregoire, S. Bonnabel, and A. De La Fortelle, "Priority-based coordination of robots," 2014.

[5] L. Makarem and D. Gillet, "Fluent coordination of autonomous vehicles at intersections," in *Systems, Man, and Cybernetics (SMC), 2012 IEEE International Conference on*. IEEE, 2012, pp. 2557–2562.

[6] T. Sakaguchi, A. Uno, and S. Tsugawa, "An algorithm for merging control of vehicles on highways," in *Intelligent Robots and Systems, 1997. IROS'97., Proceedings of the 1997 IEEE/RSJ International Conference on*, vol. 3. IEEE, 1997, pp. V15–V16.

[7] A. I. M. Medina, N. Van De Wouw, and H. Nijmeijer, "Automation of a t-intersection using virtual platoons of cooperative autonomous vehicles," in *Intelligent Transportation Systems (ITSC), 2015 IEEE 18th International Conference on*. IEEE, 2015, pp. 1696–1701.

[8] E. Debada, L. Makarem, and D. Gillet, "Autonomous coordination of heterogeneous vehicles at roundabouts," in *Intelligent Transportation Systems (ITSC), 2016 IEEE 19th International Conference on*. IEEE, 2016, pp. 1489–1495.

[9] G. R. de Campos, P. Falcone, R. Hult, H. Wymeersch, and J. Sjöberg, "Traffic coordination at road intersections: Autonomous decision-making algorithms using model-based heuristics," *IEEE Intelligent Transportation Systems Magazine*, vol. 9, no. 1, pp. 8–21, 2017.

[10] Y. Wu, Z. Zhang, J. Yuan, Q. Ma, and L. Gao, "Sequential game solution for lane-merging conflict between autonomous vehicles," in *Intelligent Transportation Systems (ITSC), 2016 IEEE 19th International Conference on*. IEEE, 2016, pp. 1482–1488.

[11] A. De La Fortelle and X. Qian, "Autonomous driving at intersections: combining theoretical analysis with practical considerations," in *ITS World Congress 2015*, 2015.

[12] V. Milanés, J. Godoy, J. Villagrá, and J. Pérez, "Automated on-ramp merging system for congested traffic situations," *IEEE Transactions on Intelligent Transportation Systems*, vol. 12, no. 2, pp. 500–508, 2011.

[13] M. Treiber and A. Kesting, "Car-following models based on driving strategies," in *Traffic Flow Dynamics*. Springer, 2013, pp. 181–204.

[14] V. V. Dixit, "Modeling origin-destination effects on roundabout operations and inflow control," *Journal of Transportation Engineering*, vol. 138, no. 8, pp. 1016–1022, 2011.